Ligand Binding Properties of Bacterial Hemoglobins and Flavohemoglobins†

Judith Farrés,‡ Markus P. Rechsteiner,‡,|| Susanna Herold,§ Alexander D. Frey,‡ and Pauli T. Kallio*,‡

Institute of Biotechnology and Laboratory of Inorganic Chemistry, Eidgenössiche Technische Hochschule Zürich, CH-8093 Zürich, Switzerland

Received December 13, 2004

ABSTRACT: Bacterial hemoglobins and flavohemoglobins share a common globin fold but differ otherwise in structural and functional aspects. The bases of these differences were investigated through kinetic studies on oxygen, carbon monoxide, and nitric oxide binding. The novel bacterial hemoglobins from *Clostridium perfringens* and *Campylobacter jejuni* and the flavohemoglobins from *Bacillus subtilis* and *Salmonella enterica* serovar Typhi have been analyzed. Examination of the biochemical and ligand binding properties of these proteins shows a clear distinction between the two groups. Flavohemoglobins show a much greater tendency to autoxidation compared to bacterial hemoglobins. The differences in affinity for oxygen, carbon monoxide, and nitric oxide between bacterial hemoglobins and flavohemoglobins are mainly due to differences in the association rate constants. The second-order rate constants for oxygen and carbon monoxide binding to bacterial hemoglobins are severalfold higher than those for flavohemoglobins. A similar trend is observed for NO association with the oxidized iron(III) form of the proteins. No major differences are observed among the values obtained for the dissociation rate constants for the two groups of bacterial proteins studied, and these constants are all rather similar to those for myoglobin. Taken together, our data suggest that differences exist between the mechanisms of ligand binding to bacterial hemoglobins and flavohemoglobins, suggesting different functions in the cell.

Globins are proteins that contain a heme B prosthetic group located in a highly conserved α-helical "globin fold". Myoglobin (Mb)[1] and hemoglobin are the most well-known examples of this class of proteins, which has now been established to occur widely also in prokaryotes. On the basis of structural differences, three types of such globins have been identified so far: bacterial hemoglobins (bacterial Hbs), truncated hemoglobins (trHbs), and flavohemoglobins (flavoHbs), the latter being the most widely distributed in bacteria and fungi (*1*).

The tertiary structure of bacterial Hbs consists of seven α-helical regions adopting the three-on-three helical sandwich motif "globin fold" (*2*). FlavoHbs comprise two domains: an N-terminal globin domain and a reductase domain having a flavin adenine dinucleotide- (FAD-) and a reduced nicotinamide adenine dinucleotide (phosphate)- [NAD(P)H-] binding site (*3*). This domain belongs to the ferredoxin−NAD(P)$^+$ reductase family of proteins (*4*). The amino acid sequences of TrHbs are 20−40 residues shorter than those of bacterial Hbs and have a tertiary structure based on a two-on-two α-helical sandwich (*5*). The present study focuses on the two groups of globins that are more closely related to Mb, that is, bacterial Hbs and flavoHbs.

Detailed understanding of the biological function of these proteins remains elusive. Several possible functions have been proposed on the basis of their induction in response to oxygen limitation and/or oxidative and nitrosative stress and phenotypical effects. These include the improvement of oxygen transfer to the terminal oxidases to support aerobic metabolism of cells growing at low oxygen tensions (*1*). On the other hand, the oxygen-dependent flavin reduction has been proposed to serve as an oxygen sensor (*6*). Finally, most recent reports suggest a protective role in response to oxidative and/or nitrosative stress (*7*). The flavoHb of *Escherichia coli* (HMP) has been shown to be able to catalyze the oxidation of free NO to nitrate (nitric oxide dioxygenase activity) in the presence of O_2 and NADH (*8*, *9*). Recently, Bonamore et al. (*10*) have suggested the involvement of HMP in the reduction of lipid membrane hydroperoxides.

Amino acid sequence comparisons show that vertebrate Hbs and Mbs, with exception of elephant Mb, have His and Leu at the distal positions E7 and B10, respectively. The distal His forms a strong hydrogen bond with the bound O_2, thus stabilizing the oxygenated structure (*11*). In bacterial Hbs and flavoHbs the (E7)His and (B10)Leu residues are replaced by Gln and Tyr, respectively (Figure 1). Up to now, the three-dimensional structures of only one bacterial Hb, *Vitreoscilla* Hb (VHb) (*2*), and the flavoHbs of *Ralstonia*

† These experiments were supported by ETH Zurich.

* To whom correspondence should be addressed: tel 41-1-633 34 46; fax 41-1-633 10 51; e-mail kallio@biotech.biol.ethz.ch.

‡ Institute of Biotechnology.

|| Current address: University Children's Hospital of Zürich, Division of Infectious Diseases, Zürich, Switzerland.

§ Laboratory of Inorganic Chemistry.

[1] Abbreviations: flavoHb(s), flavohemoglobin(s); Hb(s), hemoglobin(s); trHb(s), truncated hemoglobin (s); Mb, myoglobin; CHb, *Campylobacter jejuni* hemoglobin; *chb*, *Campylobacter jejuni* hemoglobin gene; CpHb, *Clostridium perfringens* hemoglobin; *cphb*, *Clostridium perfringens* hemoglobin gene; HmpBs, *Bacillus subtilis* flavohemoglobin; *hmpBs*, *Bacillus subtilis* flavohemoglobin gene; hmpSt, *Salmonella enterica* serovar Typhi flavohemoglobin; *hmpSt*, *Salmonella enterica* serovar Typhi flavohemoglobin gene; HMP, flavohemoglobin of *Escherichia coli*; FHP, flavohemoglobin of *Ralstonia eutropha*; VHb, bacterial hemoglobin of *Vitreoscilla* sp.; NO, nitric oxide (nitrogen monoxide is the name recommended by the International Union of Pure and Applied Chemistry [IUPAC]).

10.1021/bi047389d CCC: $30.25
Published on Web 02/15/2005

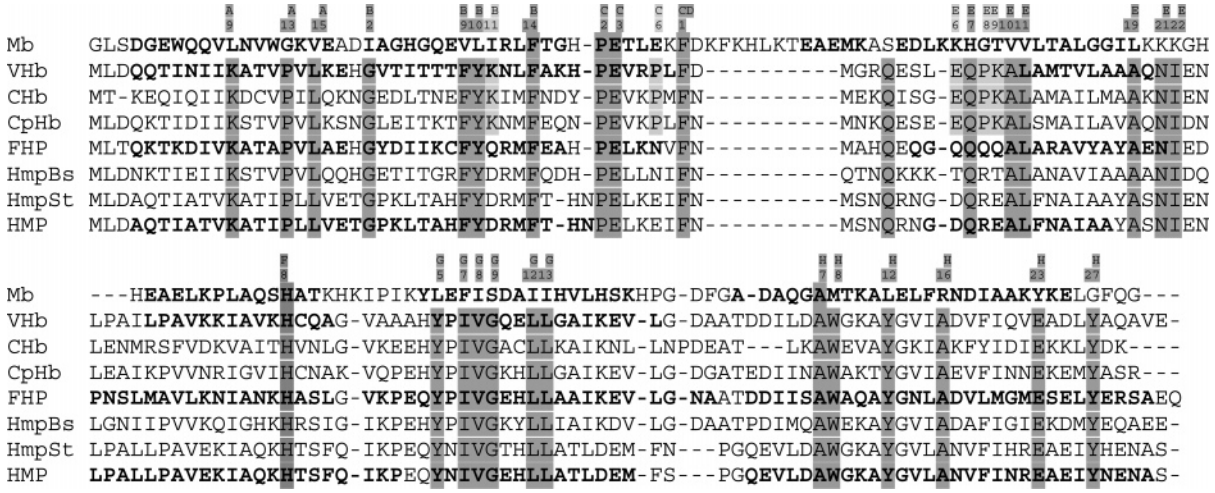

FIGURE 1: Alignment of amino acid sequences of bacterial Hb and flavoHb globin domains. Proteins characterized in the present study: *C. jejuni* Hb (CHb), *C. perfringens* Hb (CpHb), *B. subtilis* flavoHb (HmpBs), *S. enterica* serovar Typhi flavoHb (HmpSt). Sequences of Hbs and flavoHbs with known 3D structure have also been included for comparison: *Vitreoscilla* hemoglobin (VHb), *R. eutropha* flavoHb (FHP), *E. coli* flavoHb (HMP), and horse heart myoglobin (Mb). The topological positions according to the structure of Mb are annotated above the multiple alignment. α-Helical regions are shown in boldface type. Residues sharing identity between bacterial Hbs and flavoHbs are shaded in dark gray, and those sharing identity between bacterial Hbs only are shaded in light gray.

eutropha (FHP) (*3*) and *Escherichia coli* (HMP) (*12*) have been solved. The crystal structure of FHP shows tightly bound phospholipids in the heme cavity, which altered the positioning of relevant distal pocket residues, precluding any determination of protein−heme interaction at the distal site of the heme (*3*). The three-dimensional structures of the globin domains of HMP and VHb are very similar, as expected from their amino acid identity (47%). On the other hand, although HMP and VHb share only 11% and 6% amino acid identity with Mb, respectively, their tertiary structures are also closely related (rmsd 1.6 Å, excluding the D helix of Mb). This precludes any structure/function correlation based only on sequence comparisons. Therefore, investigations on the biochemical and ligand binding properties of these proteins are an essential prerequisite for the understanding of their biological roles and can reveal new aspects of heme chemistry.

The focus of the present study is comparative analysis of the rate constants for the reactions of bacterial Hbs and flavoHbs with different ligands. The novel Hbs from *Clostridium perfringens* (CpHb) and *Campylobacter jejuni* (CHb) have been used as representatives of the bacterial Hb group, and the flavoHbs from *Bacillus subtilis* (HmpBs) and *Salmonella enterica* serovar Typhi (HmpSt) as representatives of the flavoHb group. We report the kinetic data of the reactions of oxygen and carbon monoxide binding to the iron(II) form of the proteins and nitric oxide binding with the iron(II) and iron(III) forms of the proteins. This study provides a comparative insight into the ligand binding properties of two groups of proteins and discusses possible implications for their function.

EXPERIMENTAL PROCEDURES

Cloning and Expression of Hbs and FlavoHbs. Genomic DNA for PCR amplification of *cphb* Hb gene was isolated from *C. perfringens* NCIMB8875 and the strains *C. jejuni*, *B. subtilis*, and *S. enterica* serovar Typhi have been described previously (*13*). Oligonucleotide primers were designed to incorporate *Eco*RI and *Bam*HI restriction sites at the 5′- and 3′-ends of the genes, respectively, with the exception of *B. subtilis* (*hmpbs*) were *Mun*I and *Bam*HI restriction sites were used. *C. perfringens* (*cphb*) and *C. jejuni* (*chb*) Hb genes were amplified by use of oligo pairs JFM15&16 (JFM15, 5′-CGGAATTCATGTTAGATCAAAAGAC-3′, and JFM16, 5′-CGGAATTCTCTTGAACGATACAT-3′) and JFM3&4 (JFM3, 5′-CGGAATTCATGACA AAAGAAC-3′, and JFM4, 5′-CGGGATC**C**TTTATCATAGAGC-3′), respectively. *B. subtilis* (*hmpBs*) and *S. enterica* (*hmpSt*) flavohemoglobin genes were amplified by use of oligos JFM9&10 (JFM9, 5′- CGCAATTGATGTTAGATAACAAAACAATCG-3′, and JFM10, 5′- CGGGATCC AAC GGA CTG CGC CA-3′) and JFM1&2 (JFM1, 5′-CGGAATTCATGCTTGACGC-3′, and JFM2, 5′-CGGAATTCCAGCACCTTAT-3′), respectively. All PCR-amplified hemoglobin and flavohemoglobin genes were introduced into pHIS expression vector and transformed into *E. coli* XL1-Blue (*recA1 endA1 gyrA*96 *thi-1 hsdR17 supE44 relA1 lac* [F′ *proAB lacI*^{q}ZΔ*M15* Tn10 (Tet^{r})]; Stratagene) by standard techniques (*14*). pHIS is a derivative of pKQV4 (*15*) carrying a *Sph*I and *Hin*dIII fragment from pETR247 (obtained from Dr. P. Brünker, GlycArt Biotechnology, Schlieren, Switzerland). The *Sph*I−*Hin*dIII fragment contains the P_{tac} promoter, a multiple cloning site, and a DNA sequence coding for six His residues (so-called His tag). DNA sequencing was performed as described previously (*16*, *17*). The *cphb* gene reveals nucleotide substitutions relative to the GenBank-deposited sequence (*C. perfringens* str. 13, Accession Number AB028630) leading to one amino acid substitution, Ala^{57} to Ser. This substitution has been confirmed by sequencing three independent amplifications of the Hb gene from *C. perfringens* NCIMB8875. The gene sequences of other Hb (AL139079) and flavoHb genes (AB024563 and AL627275) were identical with the gene sequences deposited in GenBank. Expression vectors were transformed into *E. coli* MG1655 (F^{-} λ^{-}; Cold Spring Harbor Laboratory) for production of Hb and flavoHb proteins. All Hb and flavoHb proteins produced from the pHIS vector

contained a sequence of eight extra amino acids, GSHHHHHH, at the C-terminus, two of which, Gly and Ser, are derived from the *Bam*HI restriction site.

Production and Purification of Hbs and FlavoHbs. Globin-expressing *E. coli* cultures were grown in shake flasks at 37 °C and at 200 rpm for 4 h followed by a period of 10 h at 100 rpm, on Luria−Bertani (LB) medium (*14*) supplemented with 100 mg L^{-1} ampicillin. Cells from total of 3 L of culture were harvested, resuspended in 100 mM potassium phosphate buffer, pH 7.0, containing 1 μM phenylmethanesulfonyl fluoride (PMSF) to reach an $OD_{600} = 600$, and lysed in a French press (SLM-Aminco). All protein purification steps were performed at 4 °C. Lysates were clarified by centrifugation and filtration (0.45 μm). His-tagged Hb and flavoHb proteins were purified on an affinity column, Sephadex HisTrap chelating column (Amersham Pharmacia Biotech), and eluted stepwise in imidazole buffer (40 and 300 mM imidazole in 100 mM potassium phosphate buffer, pH 7.0) followed by a desalting column (Sephadex G25). Sample purity was estimated to be >95% for bacterial Hbs and >90% for flavoHbs from SDS−12% polyacrylamide gels (*18*) stained in Coomassie Brillant Blue. Lyophilized horse heart myoglobin was obtained from Sigma and prepared as described previously (*19*).

Heme and protein contents were assayed as described previously (*20*). FAD content was assayed by releasing FAD from flavoHb by boiling the purified protein sample for 3 min and determining the fluorescence at 520 nm with excitation at 460 nm, by comparison with pure FAD as a standard.

Preparation of Ligand-Bound Hemoglobins. Solutions of the oxygenated forms of bacterial Hb and of Mb were prepared by reducing the proteins with a slight excess of sodium dithionite and by purifying the resulting mixtures over a PD-10 column (Amersham Pharmacia Biotech). The concentrated protein stock solutions were diluted in sealed cells or in gastight SampleLock Hamilton syringes with phosphate buffer containing the required O_2 concentration. Solutions of the oxygenated forms of flavoHbs were generated in sealed cells or gastight SampleLock Hamilton syringes by adding, immediately before the measurements, NADH (400 μM, final concentration) to a solution containing the iron(III) form of the corresponding flavoHbs and the required O_2 concentration. Because of the NADH oxidase activity of these proteins, these solutions were used within 5 min. Older solutions were discarded.

The CO-bound form of the proteins was prepared by flushing concentrated protein stock solutions with argon for 15 min, adding sodium dithionite (approximately 2−5 equiv), and finally diluting the resulting mixtures with CO-saturated buffer. This stock solution was then diluted in sealed cells or gastight SampleLock Hamilton syringes with phosphate buffer containing different CO concentrations. For the preparation of MbFe(II)CO solutions needed for the determination of the rate of CO dissociation, in some cases the concentrated solution was purified over a PD-10 column (Amersham Pharmacia Biotech) equilibrated with CO-saturated buffer. This procedure proved not to be necessary, since purified and dithionite-containing solutions of MbFe(II)CO gave identical CO dissociation rates.

Solutions of the iron(II)−NO form of flavoHbs were prepared by first degassing protein stock solutions in a sealed cell with argon for approximately 15 min and then diluting them with phosphate buffer containing different concentrations of NO. Finally, the required amount of an anoxic NADH solution was added to obtain a final concentration of 400 μM.

Dithionite-free solutions of the iron(II)−NO form of Mb were obtained by reductive nitrosylation. For this purpose, a concentrated metMb solution in 0.1 M phosphate buffer, pH 8.0, was thoroughly degassed (for several hours) and then treated with an excess of NO, added from a saturated NO solution (prepared also in 0.1 M phosphate buffer, pH 8.0). The complete conversion of MbFe(III)NO to MbFe(II)NO was confirmed by UV−vis spectroscopy. The resulting MbFe(II)NO solution was degassed to remove excess NO and then diluted with 0.1 M phosphate buffer, pH 7.0, containing the NO concentration required for the laser flash photolysis experiments.

Despite the fact that we tried different procedures, it proved impossible to prepare stable solutions containing the iron(II)−NO form of bacterial Hbs. Neither the reductive nitrosylation procedure used for obtaining of MbFe(II)NO nor the replacement of the coordinated CO with excess NO led to the formation of the iron(II)−NO form, as confirmed by UV−vis spectroscopy. Alternatively, we prepared the iron(II)−NO forms of bacterial Hbs by first reducing the corresponding concentrated iron(III) protein solutions with sodium dithionite (6−15 equiv were needed, giving a final concentration in the range 55−200 μM) in sealed degassed cells (flushed for 15 min with argon). The resulting mixtures were then diluted with phosphate buffer containing the required NO concentration. Unexpectedly, despite the strict anaerobic conditions (and the presence of an excess of dithionite), the iron(II)−NO protein solutions were stable only for 10−30 min and slowly oxidized to the corresponding iron(III)−NO form. Moreover, dithionite and/or the products derived from its decomposition interfered with the laser flash photolysis measurements (see below). For comparison, Mb iron(II)−NO solutions were also prepared according to this procedure.

Solutions of the iron(III)−NO form of the proteins were prepared by diluting a thoroughly degassed iron(III) protein solution in a sealed cell with buffer containing the required NO concentration.

NADH Oxidation Rate. Measurements were performed at 20 °C with an Applied Photophysics SX18MV-R single-wavelength stopped-flow instrument. Stock solutions of the iron(III) form of flavoHbs (4−16 μM) were first diluted with buffer containing different O_2 concentrations (300−1300 μM) and then mixed in the stopped-flow instrument with an anoxic solution of NADH (100−600 μM) in buffer. NADH consumption was measured by following the absorbance decrease at 340 nm.

Association and Dissociation Rate Constants. All kinetic measurements were performed at 20 °C in 0.1 M phosphate buffer at pH 7. O_2 and CO stock solutions were prepared by equilibrating the buffer with the corresponding pure gas at room temperature. NO was prepared as described previously (*21*). If required, saturated stock solutions (1300 μM O_2, 1000 μM CO, and 2000 μM NO) were diluted with degassed buffer in gastight SampleLock Hamilton syringes. All samples were prepared immediately before use, and their

stability was checked spectrophotometrically before and after the kinetic measurements.

Association time courses for O_2, CO, and NO [($k'_{O_2}(Fe^{2+})$, $k'_{CO}(Fe^{2+})$, $k'_{NO}(Fe^{2+})$, and $k'_{NO}(Fe^{3+})$] were measured by laser flash photolysis of the ligand-bound protein samples with an Applied Photophysics LKS50 instrument fitted with a Quantel Brillian B Nd:YAG laser. Solutions were irradiated at $\lambda = 532$ or 420 nm with a pulse of 10 ns. Final protein concentrations were 2.5−10 μM. Time courses (average of 5−10 traces) were followed at two wavelengths (maximum and minimum of the differential spectra ligand-bound protein minus ligand-free protein) and measured for different ligand concentrations (O_2, 260−1300 μM; CO, 200−1000 μM; and NO, 250−2000 μM). Second-order association rate constants were obtained from the slopes of the linear plots of the observed pseudo-first-order rate constants versus ligand concentration. Averages and standard deviations of the calculated slopes are reported.

Dissociation rate constants for O_2 and CO [$k_{O_2}(Fe^{2+})$ and $k_{CO}(Fe^{2+})$] were measured directly by carrying out replacement reactions with an Applied Photophysics SX17MV or a SX18MV-R single-wavelength stopped-flow apparatus (*22*). The ligands of a 10−20 μM solution of the O_2- and CO-bound forms of the hemoproteins were replaced by a high concentration of displacing ligand (500 μM CO and 1000 μM NO, respectively). Measurements were done at two different wavelengths (maximum and minimum of the differential spectra) and at least two different ligand concentrations (65−325 μM O_2 and 50−250 μM CO). The observed rates were obtained from the fits of at least five single traces. The dissociation rate constants were then calculated from the expressions $k_{O_2} = k_{obs}(1 + k'_{O_2}[O_2]/k'_{CO}[CO])$ and $k_{CO} = k_{obs}(1 + k'_{CO}[CO]/k'_{NO}[NO])$ by using $k'_{O_2}(Fe^{2+})$, $k'_{CO}(Fe^{2+})$, and $k'_{NO}(Fe^{2+})$ determined in this work. Average values and standard deviations obtained from the different measurements are reported.

NO dissociation rate constants [$k_{NO}(Fe^{2+})$] were measured spectrophotometrically in a Cary 1E UV−vis spectrophotometer in the presence of a large excess of CO (1000 μM) and sodium dithionite (10 mM) as described previously (*23*). The progress of the dissociation was followed by recording spectra every 10 min during a 3-h period and additionally every 30 min during a further 3 h. Under these conditions, dissociation of NO is the rate-determining step, thus $k_{NO}(Fe^{2+})$ was obtained from the exponential fits of the kinetic traces at 420 and 537 nm (of three independent measurements). Mean values and standard deviations are reported.

RESULTS

Hb and FlavoHb Protein Production. Bacterial Hbs and flavoHbs were engineered to contain a His_6 tag at the C-terminus to facilitate protein purification. Identical functional behavior of His_6-tagged and nontagged Hbs has previously been reported (*24*).

Approximately 3.3, 2.6, 2.8, and 2.4 mg of purified protein/g of wet cell pellet were obtained for CHb, CpHb, HmpBs, and HmpSt, respectively. Protein purities were approximately 90−95% as estimated from SDS−PAGE gels. Purified flavoHbs were partially lacking FAD. The molar ratios of FAD to heme were 0.26 and 0.54 for HmpBs and HmpSt, respectively. FAD deficiency in purified flavoHbs has previously been reported (*25*, *26*). FAD was supplemented in all reactions to have equimolecular amounts of heme and FAD.

Table 1: Spectroscopic Data for the Iron(II), Iron(III), and Complexed Forms of the Different Hemoproteins

	λ_{max} (nm)		
protein form	Soret	visible	visible
CHb(Fe^{2+})	431	555	
CpHb(Fe^{2+})	431	554	
HmpBs(Fe^{2+})	432	555	
HmpSt(Fe^{2+})	433	558	
CHb(Fe^{3+})	401	504	625
CpHb(Fe^{3+})	406	526	631
HmpBs(Fe^{3+})	403	495	642
HmpSt(Fe^{3+})	403	498	shoulder
CHb(Fe^{2+})O_2	412	540	577
CpHb(Fe^{2+})O_2	411	539	576
HmpBs(Fe^{2+})O_2	413	540	575
HmpSt(Fe^{2+})O_2	414	542	574
CHb(Fe^{2+})CO	419	539	566
CHb(Fe^{2+})CO	418	538	565
HmpBs(Fe^{2+})CO	420	539	565
HmpSt(Fe^{2+})CO	421	540	564
CHb(Fe^{2+})NO	417	545	shoulder
CpHb(Fe^{2+})NO	417	547	shoulder
HmpBs(Fe^{2+})NO	414	545	shoulder
HmpSt(Fe^{2+})NO	417	547	shoulder
CHb(Fe^{3+})NO	418	532	566
CpHb(Fe^{3+})NO	418	530	565
HmpBs(Fe^{3+})NO	417	533	567
HmpSt(Fe^{3+})NO	421	535	569

Spectral Characterization and Stability. Spectral characterization and information on the stability of the different bacterial globins were required to study kinetics of ligand binding. The absorbance maxima for the five protein forms of the different proteins relevant for our studies are summarized in Table 1. The bacterial globins investigated displayed similar spectra, resembling that of Mb. The absorbance spectra of the iron(II) forms, which all display a single broad band near 556 nm, suggest that the reduced forms of these proteins are pentacoordinated. A similar environment is found in Mbs, in contrast to the trHb of *Synechocystis* sp. or neuroglobin and cytoglobin (also know as histoglobin) (*27*−*29*), in which a histidine residue occupies the sixth coordination site.

The oxygenated forms of the bacterial Hbs were stable for several hours at room temperature in air-equilibrated buffer, pH 7. The only characterized bacterial Hb so far, VHb, has a similar stability (*30*). In contrast, under the same conditions oxygenated forms of flavoHbs were only observable while NADH was present. Such behavior has already been observed for other flavoHbs. *E. coli* flavoHb (HMP) has been shown to consume O_2 and yield reactive oxygen species, with the concomitant oxidation of NADH (*31*−*33*). The aerobic NADH oxidation rate by the flavoHbs of the present study was also determined. HmpBs and HmpSt reported NADH oxidase activities of 0.18 ± 0.02 s^{-1} and 0.25 ± 0.02 s^{-1}, respectively. Our values are in good agreement with previously published values for HMP (0.2 s^{-1}) (*25*).

Determination of Association and Dissociation Rate Constants. Ligand association rate constants were measured by laser flash photolysis. Time courses were followed at two wavelengths (maximum and minimum of the differential

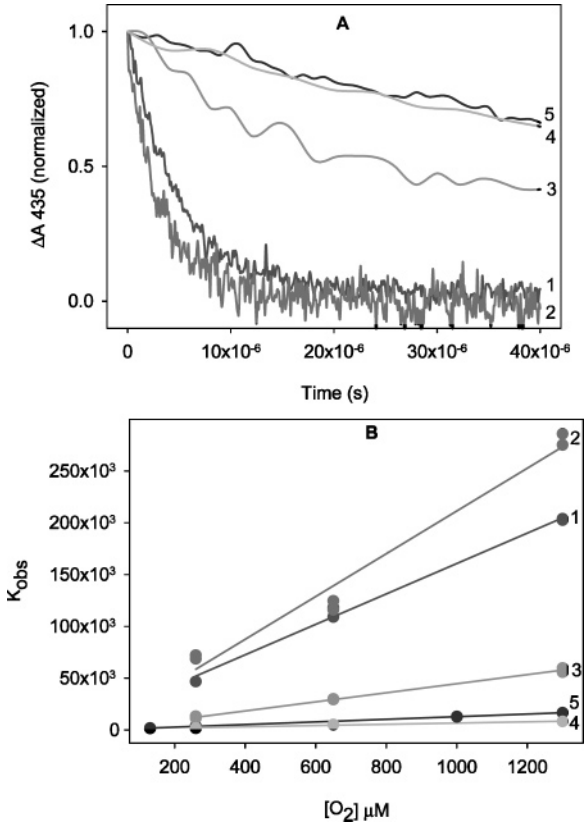

FIGURE 2: O_2 recombination kinetics after laser flash photolysis. (A) Time courses for O_2 rebinding to bacterial Hbs, flavoHbs, and Mb after laser flash photolysis in the presence of 1300 μM O_2. To facilitate comparison of the data for the various proteins, the absorbance changes were normalized to 1 at the maximum absorbance. (B) Plot of the observed rate constants for O_2 rebinding to the different proteins versus O_2 concentration. The results of the linear fits, displayed as solid lines, are given in Table 2. Lines: (1) CHb; (2) CpHb; (3) HmpBs; (4) HmpSt; (5) Mb. Protein concentrations were 2−10 μM in 0.1 M sodium phosphate buffer, pH 7.0; T = 20 °C.

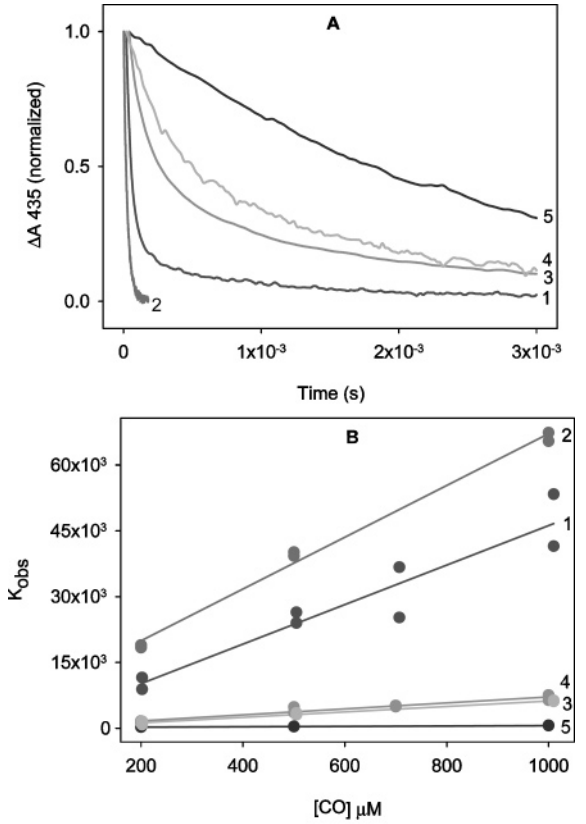

FIGURE 3: CO recombination kinetics after laser flash photolysis. (A) Time courses for CO rebinding to bacterial Hbs, flavoHbs, and Mb after laser flash photolysis in the presence of 500 μM CO. To facilitate comparison of the data for the various proteins, the absorbance changes were normalized to 1 at the maximum absorbance. (B) Plot of the observed rate constants for CO rebinding to the different proteins versus CO concentration. The results of the linear fits, displayed as solid lines, are given in Table 2. Lines: (1) CHb; (2) CpHb; (3) HmpBs; (4) HmpSt; (5) Mb. Protein concentrations were 2−10 μM in 0.1 M sodium phosphate buffer, pH 7.0; T = 20 °C.

spectra ligand-bound protein minus ligand-free protein) and measured for different ligand concentrations. For control, all measurements were also carried out with horse heart myoglobin. Typical time courses of O_2, CO, and NO recombination to Mb and to novel bacterial Hbs and flavoHbs after laser flash photolysis are shown in Figures 2A, 3A, and 4. In most cases, these traces could be fitted well with a single-exponential expression. However, time courses for oxygen association to HmpBs were biphasic; the fast phase accounted for approximately 75% of the reaction. Three of the four bacterial globins studied displayed biphasic time courses for CO rebinding. The relative amplitudes of the two phases varied among the different proteins. The fast phase accounted for approximately 85% of the reaction with CHb and 50% of that with HmpSt. In contrast, for HmpBs the percentage varied depending on the observation wavelength: at 437 nm the fast phase accounted for 70% of the reaction, while at 419 nm the fast phase was reduced to 53%. Biphasic time courses were also observed for NO rebinding to the iron(III) forms of CHb and of CpHb, with 57% and 85% of the proteins reacting faster, respectively.

Second-order association rate constants (k') for each ligand were obtained from the slopes of the linear fits of the observed rate constants (k_{obs}) versus ligand concentration, as shown for O_2 and CO in Figures 2B and 3B, respectively. The measured k' values are summarized in Table 2. In all cases, the two bacterial Hbs have comparable rates and differ from the values of the two flavoHbs, which are also comparable with each other. The second-order rate constants for O_2 and CO binding to bacterial Hbs are larger than those for binding to flavoHbs are. The rate constants for NO binding to the iron(III) forms of the proteins are also larger for bacterial Hbs compared to flavoHbs.

The association rate constants for NO binding to the iron(II) form of bacterial Hbs could not be established. As described in the section Experimental Procedures, the iron(II)−NO form of these proteins could only be prepared in the presence of a large excess of dithionite. Surprisingly, even under these condition the iron(II)−NO form of bacterial Hbs was not stable and was slowly (10−30 min) converted to the corresponding iron(III)−NO form, despite the strictly anoxic conditions. Great care was taken to ensure no O_2 contamination and, in fact, Mb samples prepared accordingly were stable. Attempts were made to carry out laser flash photolysis experiments with these dithionite-containing solutions immediately after preparation. However, the data were not reproducible, not only because of the instability of the iron(II)−NO form of these proteins but possibly also because

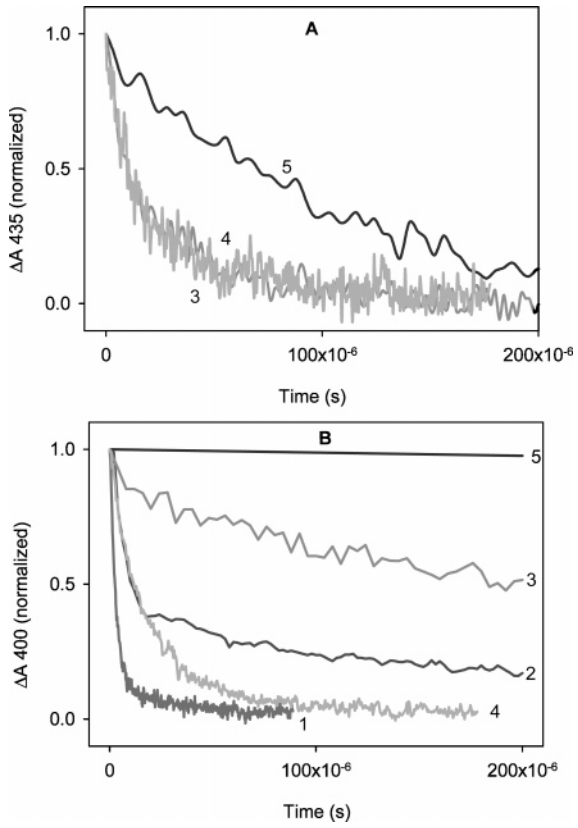

FIGURE 4: NO recombination kinetics after laser flash photolysis. (A) Time courses for NO rebinding to iron(II) form of flavoHbs and Mb after laser flash photolysis in the presence of 1000 μM NO. (B) Time courses for NO rebinding to iron(III) form of bacterial Hbs, flavoHbs, and Mb after laser flash photolysis in the presence of 1000 μM NO. To facilitate comparison of the data for the various proteins, the absorbance changes were normalized to 1 at the maximum absorbance. Lines: (1) CHb; (2) CpHb; (3) HmpBs; (4) HmpSt; (5) Mb. Protein concentrations were 2−10 μM in 0.1 M sodium phosphate buffer, pH 7.0; $T = 20$ °C.

of the presence of dithionite and/or products of its decomposition. Indeed, laser flash photolysis experiments with dithionite-containing MbFe(II)NO solutions led to a lower value of the association rate than those obtained with dithionite-free MbFe(II)NO solutions, prepared by reductive nitrosylation (see Experimental Procedures). Experiments performed in the presence of different dithionite concentrations showed a clear inverse correlation between the observed association rate constants and the amount of dithionite added (results not shown).

For all ligands studied, the values of the association rate constants for flavoHbs are always between those for Mb and those for bacterial Hbs. Previously characterized bacterial Hbs and flavoHbs (Table 2) display comparable association rate constants and follow the same tendency (*25*, *34*−*36*). Only the values of VHb CO association rate constant and VHb O_2 dissociation rate constant determined by Orii and Webster (*34*) differ significantly from the values obtained. However, not only are the methods used in the determination of these rate constants different from those used for the characterization of the other bacterial globins but also they are indirect methods. In a more recent study Giangiacomo et al. (*35*) report values of 4.2 s^{-1} and 0.15 s^{-1} for the fast and slow phases of VHb O_2 dissociation rate constant measured by a method similar to that used in this study and in further investigations of other flavoHbs (*25*, *36*). These values are in agreement with those reported here for CHb and CpHb.

Since dissociation rate constants (k) were mostly very small, they were determined independently by stopped-flow spectroscopy, for better accuracy. $k_{O_2}(Fe^{2+})$ and $k_{CO}(Fe^{2+})$ were determined by ligand displacement with CO and NO, respectively. Typical time courses for these reactions are shown in Figure 5. Most kinetic traces could be fitted well with a single-exponential expression. However, O_2 dissociation from HmpBs and from HmpSt was biphasic; the fast phase accounted for 75% and 61%, respectively, of the reaction. k values were calculated from observed displacement rates as described under Experimental Procedures. NO dissociation from the iron(II) forms of Hbs and flavoHbs was measured spectrophotometrically after addition of an excess of sodium dithionite and CO. Spectra were taken at regular intervals to ensure that initially the proteins were in the iron(II)−NO form and to follow the progress of the reaction. Progress of NO dissociation at the Soret maximum for the different proteins studied is shown in Figure 6. All k values for the different ligands studied are summarized in Table 2. In contrast to the association rate constants, no clear difference between flavoHbs and bacterial Hbs dissociation rate constants are observed. The rate of dissociation from iron(II) form decreases in the order $O_2 > CO > NO$, as in most native myoglobins.

Kinetic studies of previously characterized flavoHbs, as well as other studies on Mb mutants (*37*) and hexacoordinated Hbs (*38*), also reported that ligand association and dissociation kinetics are sometimes biphasic. No clear explanation was generally given for this behavior, which may be due to the presence of different conformations of the heme pocket, possibly as a result of a higher conformational flexibility. In addition, in flavoHbs the reaction can be complicated by additional interactions with the reductase domain, leading to different extents of reduction (*25*).

Interestingly, we found that the dissociation rate of CO from MbFe(II)CO, determined by NO replacement, depended on the concentration of the protein and on the wavelength chosen to follow the reaction. Moreover, in some cases the traces were also biphasic. Taken together, these results suggest that dissociation of CO from MbFe(II)CO is a process more complex than previously reported.[2] The value reported in Table 2 was measured under conditions similar to those used for determination of the dissociation constants of the bacterial Hbs and flavoHbs; that is, with a protein concentration of ca. 3 μM and by following the absorbance changes at the absorbance maximum of the corresponding iron(II)−CO form.

The equilibrium constants calculated from the association and dissociation rates show that, as with most Mbs, the increasing overall ligand affinity going from O_2 to CO to NO is largely due to a decrease of the dissociation rate constant. However, in general the O_2, CO, and NO affinities of bacterial Hbs and flavoHbs are much higher than those of Mb.

[2] Details on these studies are outside the scope of this work and will be published elsewhere.

Table 2: Kinetic Binding Constants of Bacterial Hemoglobins and Flavohemoglobins[a]

	$(Fe^{2+})O_2$		$(Fe^{2+})CO$		$(Fe^{2+})NO$		$(Fe^{3+})NO$		
protein	k' (μM^{-1} s^{-1})	k (s^{-1})	k' (μM^{-1} s^{-1})	k (10^{-2} s^{-1})	k' (μM^{-1} s^{-1})	k (10^{-4} s^{-1})	k' (μM^{-1} s^{-1})	k (s^{-1})	ref
Mb	13 ± 0.3	11 ± 3	0.5 ± 0.1	15 ± 1 (8.0 ± 0.2)	21 ± 1	1.1 ± 0. 3	0.044 ± 0.005	ND	this work
HMP	38	0.44	22[b] (1.4, 0.3−0.5)	5.7[c] (1.8)	26[b] (4)	2	44[b] (5.8)	~4000	*36*, *25*
FHP	50	0.2	0.11	8[b]	10−20[b]	ND	2.4	1200	*25*
HmpBs	44[b] ± 4 (2.8)	7[b] ± 2 (0.3)	7[d] ± 2 (0.5)	36 ± 7	38 ± 4	2.1 ± 0. 5	2.4 ± 0.4	ND	this work
HmpSt	6 ± 1	1.5[c] ± 0.1 (0.08)	6[c] ± 1 (0.9)	6.23 ± 0.04	42 ± 13	3.4 ± 0.3	48 ± 3	ND	this work
VHb	78	5600	0.0007	16	ND	ND	ND	ND	*34*
VHb	200	4.2[e] ± 0.2 (0.15 ± 0.04)	ND	ND	ND	ND	ND	ND	*35*
CHb	154 ± 17	1.1 ± 0.1	45[a] ± 17 (1.9)	40 ± 20	ND	1.6 ± 0.5	133[c] ± 26 (4)	ND	this work
CpHb	207 ± 40	1.8 ± 0.2	59 ± 5	30 ± 10	ND	6 ± 2	312[a] ± 66 (26)	ND	this work

[a] Rate constants for O_2, CO, and NO association (k') and dissociation (k) were measured at 20 °C, 0.1 M phosphate buffer, and pH 7.0 as described under Experimental Procedures. Errors for k' are the standard deviations from the slopes of plots of the observed pseudo-first-order rate constants versus ligand concentration. Errors for k are standard deviations from the mean of at least three independent measurements. ND, not determined. [b] Reactions were biphasic. The fast phase accounts for 70% or more of the reaction. The slow rate is reported in parentheses. [c] Reactions were biphasic. The fast rate accounts for 50% or more of the reaction. The slow rate is reported in parentheses. [d] Reactions were biphasic. The fast rate accounts for approximately 70% of the reaction when measured at 437 nm and for approximately 50% when measured at 419 nm. The slow rate is reported in parentheses. [e] Reactions were biphasic. The fast rate accounts for 15% of the reaction. The slow rate is reported in parentheses.

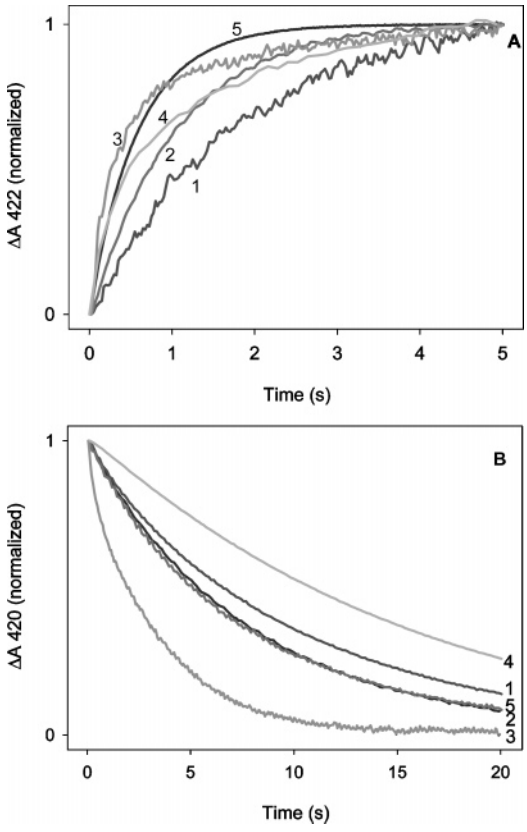

FIGURE 5: O_2 and CO dissociation time courses measured by stopped-flow. (A) Time courses for O_2 displacement by CO ([O_2] = 130 μM), [CO] = 500 μM). (B) Time courses for CO displacement by NO ([CO] = 100 μM, [NO] = 1000 μM). Lines: (1) CHb; (2) CpHb; (3) HmpBs; (4) HmpSt; (5) Mb. Protein concentrations were 10−20 μM in 0.1 M sodium phosphate buffer, pH 7.0; T = 20 °C.

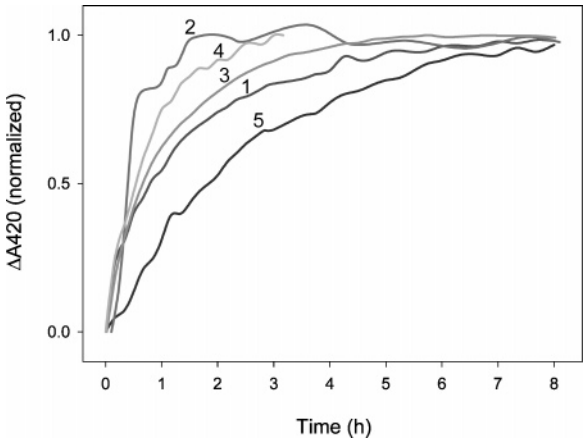

FIGURE 6: NO Dissociation time courses from iron(II) Hbs and flavoHbs. Protein samples, 2−5 μM of the NO−iron(II) form of the proteins, were injected in sealed cells containing 1000 μM CO and 10 mM sodium dithionite in 0.1 M sodium phosphate buffer, pH 7.0, T = 20 °C. NO dissociation was followed spectrophotometrically. Progress of the dissociation at the Soret maximum is displayed. Lines: (1) CHb; (2) CpHb; (3) HmpBs; (4) HmpSt; (5) Mb.

DISCUSSION

Among the different classes of globins existing in bacteria, bacterial Hbs and flavoHbs have been suggested to have a similar function and to serve as nitric oxide dioxygenases. This hypothesis is based on the high similarity between the structures of their globin domains (*12*). However, a detailed examination of the biochemical and ligand binding properties of these proteins shows a clear distinction between the two groups.

The first clear difference between the two types of proteins is the autoxidation rate. FlavoHbs show a much greater tendency to autoxidize than bacterial Hbs. In fact, flavoHbs were purified in the iron(III) form and could be kept in the oxygenated form only in the presence of a reducing agent. Previously characterized flavoHbs have been shown to consume O_2 and yield reactive oxygen species, with the concomitant oxidation of NADH (*25*, *32*). The NADH oxidase activities of the flavoHbs HmpBs and HmpSt are

similar to those reported for *E. coli*, *R. eutropha*, and *Saccharomyces cerevisiae* flavoHbs (*25*), autoxidizing within minutes. Therefore, it would be plausible that flavoHbs have evolved a reductase domain to overcome the susceptibility to autoxidation of their globin domains, thus suggesting that for biological function they are in the reduced forms. However, the autoxidation rate of the flavoHb from the yeast *Candida norvegensis* is comparable to those of bacterial Hbs, being stable for some hours (*26*). Although the oxygenated forms of bacterial Hbs are more stable than those of flavoHbs, the autoxidation rates of both types of proteins are still higher relative to Mbs. It has been shown that the globin moiety plays an important role for the stabilization of the FeO_2 unit. Mb has evolved with a heme cavity that can protect the FeO_2 center from easy access of a water molecule and its conjugate ions (OH^- and H^+) (*39*). The higher autoxidation rate of flavoHbs can be due to a higher solvent accessibility to the active site. The heme cavity in flavoHbs is much bigger than that of Mb and bacterial Hbs, as predicted by use of the software CastP (*40*).

Ligand affinity constants also show a clear distinction between the two groups of bacterial globins. The O_2 and CO affinity constants and the rates of NO binding to the iron(III) forms of the proteins are higher in bacterial Hbs compared to flavoHbs. All, bacterial Hbs and flavoHbs characterized so far have higher O_2, CO, and NO affinities than Mb. Studies on vertebrate Mbs show that two major factors affect the rate of ligand entry into the protein. In wild-type deoxy-Mb a noncoordinated water molecule hydrogen-bonds to the N^{ϵ} atom of the distal His(E7) and has to be displaced before ligand binding. Stabilization of this water molecule in the interior of the distal pocket of the deoxyMb causes a decrease of the association rate constants for all ligands (*41*). It has also been shown that the size and depth of the distal pocket is a major determinant of the rate of ligand entry into the protein: a decrease in the size of the pocket causes a reduction in the rate of ligand entry. In contrast, the ligand release depends more on the frequency of upward and outward movements of the distal histidine, as well as the number and the accessibility of the internal cavities (*42*). The three-dimensional structures of the bacterial globins used in this study are not yet available. In an attempt to correlate the ligand binding properties with the molecular structures, we compare our present findings with structural data available for bacterial globins, that is, the flavoHb HMP and the bacterial Hb of *Vitreoscilla* (VHb). It is expected that the structures of these proteins are rather similar to those in the present study. The three-dimensional structures of HMP and VHb show that the E7 residue, a glutamine, does not play a significant role in ligand binding to the heme of these proteins. A Gln(E7)Leu substitution in VHb had little effect on ligand binding properties (*43*). In fact, in both VHb and HMP, the Gln(E7) side chain does not contribute to the formation of the first distal pocket shell in the unliganded derivatives (*12*). Another key residue for the regulation of ligand binding in Mb is the distal Val(E11). Interestingly, Leu replacement, the corresponding amino acid present in bacterial hemoglobins and flavohemoglobins at this position, does not significantly affect the tertiary structure but causes distortions of the interior spaces, resulting in net increases of the association rate constants due to the absence of the distal pocket water molecule (*44*). In addition, the percentage of nonpolar residues interacting with the heme in the distal site of VHb is higher than in Mb, as measured by use of LPC (ligand−protein contacts) software (*45*). In conclusion, compared to Mbs, a more apolar heme environment in the case of bacterial Hbs, a bigger heme cavity in the case of flavoHbs, and for both bacterial Hbs and flavoHbs the lack of water stabilization in the interior of the distal pocket can be some of the factors that contribute to the higher O_2, CO, and NO affinities of these proteins.

Significant differences between the two groups of bacterial globin proteins studied were found in their affinities for ligands. These were mainly due to differences in the association rate constants. The heme distal site of the bacterial Hb VHb and the flavoHb HMP show notable differences, despite the remarkable similarity of the overall fold of the heme domains. The topological position E8 in VHb distal site seems to be important. The proline ring at this position prevents access of the solvent or ligand to the heme distal site and is displaced upon ligand binding (*2*, *46*). The same position in HMP is occupied by an arginine residue whose side chain is oriented toward the outside of the distal pocket, while in HMP it seems that it is the isopropyl site chain of Leu(E11) which rotates to accommodate the incoming ligand (*12*). Alignment of the amino acid sequences of all characterized bacterial Hbs shows that the residues at the topological positions E6, E8, and E9 are identical in these proteins but that they differ from those of flavoHbs. It is likely that these residues are responsible for the differences in ligand affinity between bacterial Hb and flavoHbs. More structural data on bacterial globins is needed to confirm this hypothesis.

Comparison of the kinetic data makes a clear distinction between the two groups of bacterial proteins, suggesting that flavoHbs and bacterial Hbs may have different roles in the cell. Previously, it has been proposed that the NO-induced oxidation (NO dioxygenation) of flavoHbs is favored relative to Mb because of the larger O_2 association rate constant and the smaller O_2 dissociation rate constant of flavoHbs provides the relatively stable iron(II)$-O_2$ intermediate required for the reaction (*25*). According to this hypothesis, NO dioxygenation would be more favored in bacterial Hbs with respect to flavoHbs because bacterial Hbs have even larger O_2 association rate constants. On the other hand, it is not known how fast the necessary rereduction step in bacterial Hbs, which relies on an external and unidentified reductase system, will proceed in vivo. Moreover, up to now only the expression of the bacterial Hb CHb has been shown to be induced under nitrosative stress (*47*). Analogously, recent studies have shown that Mb in addition to being responsible for O_2 storage and supply can act as NO oxidase and thus contribute to the attenuation of oxidative stress in cardiac muscle (*48*).

ACKNOWLEDGMENT

We thank Dr. Thomas Nauser for skillful technical assistance during laser-flash photolysis experiments.

REFERENCES

1. Frey, A. D., and Kallio, P. T. (2003) Bacterial hemoglobins and flavohemoglobins: versatile proteins and their impact on microbiology and biotechnology, *FEMS Microbiol. Rev. 789*, 1−21.

2. Tarricone, C., Galizzi, A., Coda, A., Ascenzi, P., and Bolognesi, M. (1997) Unusual structure of the oxygen-binding site in the dimeric bacterial hemoglobin from *Vitreoscilla* sp., *Structure 5*, 497−507.
3. Ermler, U., Siddiqui, R. A., Cramm, R., and Friedrich, B. (1995) Crystal structure of the flavohemoglobin from *Alcaligenes eutrophus* at 1.75 Å resolution, *EMBO J. 14*, 6067−6077.
4. Karplus, P. A., Daniels, M. J., and Herriott, J. R. (1991) Atomic structure of ferredoxin−$NADP^+$ reductase: prototype for a structurally novel flavoenzyme family, *Science 251*, 60−66.
5. Milani, M., Pesce, A., Ouellet, Y., Ascenzi, P., Guertin, M., and Bolognesi, M. (2001) *Mycobacterium tuberculosis* hemoglobin N displays a protein tunnel suited for O_2 diffusion to the heme, *EMBO J. 20*, 3902−3909.
6. Poole, R. K. (1994) Oxygen reactions with bacterial oxidases and globins: binding, reduction and regulation, *Antonie van Leeuwenhoek 65*, 289−310.
7. Poole, R. K., and Hughes, M. N. (2000) New functions for the ancient globin family: bacterial responses to nitric oxide and nitrosative stress, *Mol. Microbiol. 36*, 775−783.
8. Gardner, P. R., Gardner, A. M., Martin, L. A., and Salzman, A. L. (1998) Nitric oxide dioxygenase: an enzymic function for flavohemoglobin, *Proc. Natl. Acad. Sci. U.S.A. 95*, 10378−10383.
9. Hausladen, A., Gow, A. J., and Stamler, J. S. (1998) Nitrosative stress: metabolic pathway involving the flavohemoglobin, *Proc. Natl. Acad. Sci. U.S.A. 95*, 14100−14105.
10. Bonamore, A., Gentili, P., Ilari, A., Schinina, M. E., and Boffi, A. (2003) *Escherichia coli* flavohemoglobin is an efficient alkylhydroperoxide reductase, *J. Biol. Chem. 278*, 22272−22277.
11. Perutz, M. F. (1989) Myoglobin and haemoglobin: role of distal residues in reactions with haem ligands, *Trends Biochem. Sci. 14*, 42−44.
12. Ilari, A., Bonamore, A., Farina, A., Johnson, K. A., and Boffi, A. (2002) The X-ray structure of ferric *Escherichia coli* flavohemoglobin reveals an unexpected geometry of the distal heme pocket, *J. Biol. Chem. 277*, 23725−23732.
13. Bollinger, C. J. T., Bailey, J. E., and Kallio, P. T. (2001) Novel hemoglobins to enhance microaerobic growth and substrate utilization in *Escherichia coli*, *Biotechnol. Prog. 17*, 798−808.
14. Sambrook, J., Fritsch, E. F., and Maniatis, T. (1989) *Molecular Cloning: A laboratory manual*, Cold Spring Harbor Laboratory Press, Cold Spring Harbor, NY.
15. Strauch, M. A., Spiegelman, G. B., Perego, M., Johnson, B. C., Burbulys, D., and Hoch, J. A. (1989) The transition state transcription regulator AbrB of *Bacillus subtilis* is a DNA binding protein, *EMBO J. 8*, 1615−1621.
16. Sanger, F., Nicken, S., and Coulson, A. R. (1977) DNA sequencing with chain terminating inhibitors, *Proc. Natl. Acad. Sci. U.S.A. 74*, 5463−5467.
17. Farrés, J., and Kallio, P. T. (2002) Improved cell growth in tobacco suspension cultures expressing *Vitreoscilla* hemoglobin, *Biotechnol. Prog. 18*, 229−233.
18. Laemmli, U. K. (1970) Cleavage of structural proteins during the assembly of the head of bacteriophage T4, *Nature 277*, 680−685.
19. Herold, S., Exner, M., and Nauser, T. (2001) Kinetic and mechanistic studies of the NO*-mediated oxidation of oxymyoglobin and oxyhemoglobin, *Biochemistry 40*, 3385−3395.
20. Frey, A. D., Farrés, J., Bollinger, C. J. T., and Kallio, P. T. (2002) Bacterial hemoglobins and flavohemoglobins for alleviation of nitrosative stress in *Escherichia coli*, *Appl. Environ. Microbiol. 68*, 4835−4840.
21. Herold, S., and Rock, G. (2003) Reactions of deoxy-, oxy-, and methemoglobin with nitrogen monoxide. Mechanistic studies of the S-nitrosothiol formation under different mixing conditions, *J. Biol. Chem. 278*, 6623−6634.
22. Olson, J. S. (1981) Stopped-flow, rapid mixing measurements of ligand binding to hemoglobins and red cells, *Methods Enzymol. 76*, 631−651.
23. Moore, E. G., and Gibson, Q. H. (1976) Cooperativity in the dissociation of nitric oxide from hemoglobin, *J. Biol. Chem. 251*, 2788−2794.
24. Trent, J. T., 3rd, and Hargrove, M. S. (2002) A ubiquitously expressed human hexacoordinate hemoglobin, *J. Biol. Chem. 277*, 19538−19545.
25. Gardner, P. R., Gardner, A. M., Martin, L. A., Dou, Y., Li, T., Olson, J. S., Zhu, H., and Riggs, A. F. (2000) Nitric oxide dioxygenase activity and function of flavohemoglobins: sensitivity to nitric oxide and carbon monoxide inhibition, *J. Biol. Chem. 275*, 31581−31587.
26. Kobayashi, G., Nakamura, T., Ohmachi, H., Matsuoka, A., Ochiai, T., and Shikama, K. (2002) Yeast flavohemoglobin from *Candida norvegensis*. Its structural, spectral, and stability properties, *J. Biol. Chem. 277*, 42540−42548.
27. Scott, N. L., and Lecomte, J. T. (2000) Cloning, expression, purification, and preliminary characterization of a putative hemoglobin from the cyanobacterium *Synechocystis* sp. PCC 6803, *Protein Sci. 9*, 587−597.
28. Dewilde, S., Kiger, L., Burmester, T., Hankeln, T., Baudin-Creuza, V., Aerts, T., Marden, M. C., Caubergs, R., and Moens, L. (2001) Biochemical characterization and ligand binding properties of neuroglobin, a novel member of the globin family, *J. Biol. Chem. 276*, 38949−38955.
29. Burmester, T., Ebner, B., Weich, B., and Hankeln, T. (2002) Cytoglobin: a novel globin type ubiquitously expressed in vertebrate tissues, *Mol. Biol. Evol. 19*, 416−421.
30. Liu, C. Y., and Webster, D. A. (1974) Spectral characteristics and interconversions of the reduced oxidized, and oxygenated forms of purified cytocrome *o*, *J. Biol. Chem. 249*, 4261−4266.
31. Poole, R. K., Ioannidis, N., and Orii, Y. (1994) Reactions of the *Escherichia coli* flavohaemoglobin (Hmp) with oxygen and reduced nicotinamide adenine dinucleotide: evidence for oxygen switching of flavin oxidoreduction and a mechanism for oxygen sensing, *Proc. R. Soc. London B: Biol. Sci. 255*, 251−258.
32. Membrillo-Hernández, J., Ioannidis, N., and Poole, R. K. (1996) The flavohaemoglobin (HMP) of *Escherichia coli* generates superoxide in vitro and causes oxidative stress in vivo, *FEBS Lett. 382*, 141−144.
33. Wu, G., Corker, H., Orii, Y., and Poole, R. K. (2004) *Escherichia coli* Hmp, an "oxygen-binding flavohaemoprotein", produces superoxide anion and self-destructs, *Arch. Microbiol. 182*, 193−203.
34. Orii, Y., and Webster, D. A. (1986) Photodissociation of oxygenated cytochrome *o* (s) (*Vitreoscilla*) and kinetic studies of reassociation, *J. Biol. Chem. 261*, 3544−3547.
35. Giangiacomo, L., Mattu, M., Arcovito, A., Bellenchi, G., Bolognesi, M., Ascenzi, P., and Boffi, A. (2001) Monomer−dimer equilibrium and oxygen binding properties of ferrous *Vitreoscilla* hemoglobin, *Biochemistry 40*, 9311−9316.
36. Gardner, A. M., Martin, L. A., Gardner, P. R., Dou, Y., and Olson, J. S. (2000) Steady-state and transient kinetics of *Escherichia coli* nitric oxide dioxygenase (flavohemoglobin)−The B10 tyrosine hydroxyl is essential for dioxygen binding and catalysis, *J. Biol. Chem. 275*, 12581−12589.
37. Draghi, F., Miele, A. E., Travaglini-Allocatelli, C., Vallone, B., Brunori, M., Gibson, Q. H., and Olson, J. S. (2002) Controlling ligand binding in myoglobin by mutagenesis, *J. Biol. Chem. 277*, 7509−7519.
38. Hargrove, M. S. (2000) A flash photolysis method to characterize hexacoordinate hemoglobin kinetics, *Biophys. J. 79*, 2733−2738.
39. Shikama, K. (1998) The molecular mechanism of autoxidation for myoglobin and hemoglobin: a venerable puzzle, *Chem. Rev. 98*, 1357−1373.
40. Liang, J., Edelsbrunner, H., and Woodward, C. (1998) Anatomy of protein pockets and cavities: measurement of binding site geometry and implications for ligand design, *Protein Sci. 7*, 1884−1897.
41. Olson, J. S., and Phillips, G. N., Jr. (1996) Kinetic pathways and barriers for ligand binding to myoglobin, *J. Biol. Chem. 271*, 17593−17596.
42. Scott, E. E., Gibson, Q. H., and Olson, J. S. (2001) Mapping the pathways for O_2 entry into and exit from myoglobin, *J. Biol. Chem. 276*, 5177−5188.
43. Dikshit, K. L., Orii, Y., Navani, N., Patel, S., Huang, H. Y., Stark, B. C., and Webster, D. A. (1998) Site-directed mutagenesis of bacterial hemoglobin: the role of glutamine (E7) in oxygen-binding in the distal heme pocket, *Arch. Biochem. Biophys. 349*, 161−166.
44. Quillin, M. L., Li, T., Olson, J. S., Phillips, G. N., Dou, Y., Ikeda-Saito, M., Regan, R., Carlson, M., Gibson, Q. H., Li, H., and Elber, R. (1995) Structural and functional effects of apolar mutations of the distal valine in myoglobin, *J. Mol. Biol. 245*, 416−436.
45. Sobolev, V., Sorokine, A., Prilusky, J., Abola, E. E., and Edelman, M. (1999) Automated analysis of interatomic contacts in proteins, *Bioinformatics 15*, 327−332.

46. Bolognesi, M., Boffi, A., Coletta, M., Mozzarelli, A., Pesce, A., Tarricone, C., and Ascenzi, P. (1999) Anticooperative ligand binding properties of recombinant ferric *Vitreoscilla* homodimeric hemoglobin: a thermodynamic, kinetic and X-ray crystallographic study, *J. Mol. Biol. 291*, 637−650.

47. Elvers, K. T., Wu, G., Gilberthorpe, N. J., Poole, R. K., and Park, S. F. (2004) Role of an inducible single-domain hemoglobin in mediating resistance to nitric oxide and nitrosative stress in *Campylobacter jejuni* and *Campylobacter coli*, *J. Bacteriol. 186*, 5332−5341.

48. Flogel, U., Godecke, A., Klotz, L. O., and Schrader, J. (2004) Role of myoglobin in the antioxidant defense of the heart, *FASEB J. 18*, 1156−1158.

BI047389D